Soil Dynamics and Earthquake Engineering 106 (2018) 182–195

Contents lists available at ScienceDirect

Soil Dynamics and Earthquake Engineering

journal homepage: www.elsevier.com/locate/soildyn

Seismic design and performance of dry-assembled precast structures with adaptable joints

Bruno Dal Lago[a], Paolo Negro[b,*], Alberto Dal Lago[c]

[a] Department of Civil and Environmental Engineering, Politecnico di Milano, Milan, Italy
[b] European Commission, Joint Research Centre, Ispra, Italy
[c] DLC Consulting, Milan, Italy

ARTICLE INFO

Keywords:
Precast structures
Joint adaptation, mechanical connections
Dry joints
Seismic performance
Non-linear analysis
Full-scale testing

ABSTRACT

Previous research projects and post-earthquake field observation showed that dry-assembled precast frame structures with hinged beams and cantilever columns restrained at their base, if correctly designed and detailed, can attain good seismic performance, mainly due to their flexibility and robustness. Their seismic design is often conditioned by the need of reducing their flexibility by increasing the cross-section of the columns, which, due to minimum reinforcement requirements, results in their over-strengthening. High flexibility may also induce displacement compatibility issues with non-structural elements. The paper concerns the proposal of an innovative enhanced structural frame system, based on the adaptation of hinged beam-column joints into rigid through the activation of special mechanical connection devices performed after the installation of the slab. While keeping all the benefits of the dry prefabrication, the resulting moment-resisting frame is provided with enhanced redundancy and stiffness. A design comparison among three precast frames with similar geometries and different static schemes shows how the joint adaptation can be exploited to optimise the structure by modifying the distribution of bending moment. The results of dynamic non-linear analyses on a three-storey precast structure with adaptable joints tested as a part of the SAFECAST research programme show the seismic performance of this system through different static schemes, and the comparison with the experimental results provides information about the validity of the models and the effectiveness of the technological solutions employed.

1. Introduction

Dry-assembled precast frame structures with hinged beams and cantilever columns restrained at their base are extensively used in Europe and in several other regions of the globe mainly for single-storey or low-rise multi-storey either industrial or commercial buildings.

Wet-assembled partially precast structures are designed to emulate cast-in-situ concrete structures with rigid connections through in-situ concrete pouring of the joints, usually provided with rebars that protrude from the precast members. On the contrary, dry-assembled precast structures are connected by mechanical devices avoiding in-situ concrete pouring. Conventionally, dry-assembled joints also include semi-dry connections, which need in-situ casting of a small volume of special mortar for completion. Dry-assembled precast frame structures maximise the benefits of the prefabricated construction technique. Typical structural layouts and details of this type of structures are available in [1,2].

Over the last two decades an extensive research activity aimed at investigating the seismic behaviour of precast concrete frame structures [3] allowed a good knowledge of the seismic behaviour of precast systems to be consolidated and contributed to the achievement of outstanding realisations in terms of both quality and reliability [4]. The results from both analytical and full-scale experimental investigations showed that these precast systems (I) are characterised by an intrinsic large flexibility coming from their peculiar traditional static scheme with hinged beam-column joints [3,5–7]; (II) can provide comparable energy dissipation capacity/seismic performance as cast-in-situ systems if the connections are properly designed and drift limitations and other minimum requirements provided by structural standards are respected [3,8]; however, (III) quite often the flexibility limitation requirements govern, resulting into larger column cross-sections than those strictly needed to resist the seismic forces for the assumed global ductility level [6]; in such case, (IV) minimum reinforcement requirements impose large over-strength in the columns, so that (V) while the structures possess adequate safety levels, they often behave elastically or in the range of low ductility even under the ultimate design seismic action, not fully exploiting the energy dissipation resources of the column [6,9].

* Correspondence to: European Commission, Joint Research Centre (JRC), Via Enrico Fermi 2749, 21027 Ispra, VA, Italy.
E-mail address: paolo.negro@ec.europa.eu (P. Negro).

https://doi.org/10.1016/j.soildyn.2017.12.016
Received 31 July 2017; Received in revised form 18 November 2017; Accepted 8 December 2017
0267-7261/ © 2017 The Authors. Published by Elsevier Ltd. This is an open access article under the CC BY-NC-ND license (http://creativecommons.org/licenses/BY-NC-ND/4.0/).

This raises the problem of the capacity of the connections, in particular for multi-storey buildings [10], and the compatibility of displacements with possible interacting non-structural members, for instance the cladding panels [11–15], which caused quite extensive failures in the last strong earthquakes which hit Southern Europe [16–18]. A systematic framing of the design of precast structures including the in-plane effect of cladding panels supported by extensive experimental activity was addressed in the Safecladding project [19–25].

The seismic performance of these structures may also be influenced by the diaphragm effectiveness, since roofs often have spaced members and skylight openings. In this case, the diaphragm effect relies on the structural behaviour of the roof connections [26].

In the current European design practice [27], the key design parameters are often (i) the inter-storey drift sensitivity coefficient θ, defined as the ratio between vertical and horizontal loads at a storey divided by the inter-storey drift ratio ($\theta = P_{tot}\, d_r \,/\, V_{tot}\, h$), at Ultimate Limit State (ULS), or (ii) the drift limitation at Drift Limitation State (DLS), rather than (iii) the column base strength at ULS. To be noted that, in traditional multi-storey precast structures with hinged beam-column joints, the column strength is not influenced by the capacity design, since the beams are not part of the lateral load resisting system.

Several structural solutions were proposed to limit the flexibility of typical dry-assembled precast frame structures while keeping their dry assemblage, mainly focusing on the addition of bracers like dry-assembled precast walls [28] or diagonal metallic devices [29–31] or on the less effective introduction of rotational dissipative devices in the beam-column joints [32,33]. Solutions concerning rigid beam-column connections have been mainly developed involving in situ concrete pouring [34]. Alternative dry approaches concern “hybrid” structural arrangements based on the use of precast dry-assembled rocking frames with unbonded post-tensioning giving an elastic restoring action coupled with metallic connection devices providing dissipation of energy and hysteretic damping [35]. The use of re-centring unbonded strands and dissipative connections is the basis of the Precast Seismic Structural System (PreSSS), to which a large experimental campaign was devoted at the end of the 1990s and further [36]. Despite the results showed a large ductility associated to a low-moderate damage of the concrete components, the diffusion of this construction system in practice found difficulties, mainly due to its complexity.

Within the present paper, an innovative solution to reduce the flexibility of dry-assembled precast frame structures and improve their seismic performance is proposed, based on the adaptation of selected nodes of the frame from hinged into rigid using mechanical devices that couple the reinforcement of columns and beams avoiding any in-situ concrete pouring (Precast Structure with Adaptable Joints [37]).

2. Precast Structures with Adaptable Joints (PSAJ)

A unique structural system with variable structural configuration was conceived with beam-column and/or floor-to-beam hinged joints during assemblage, which can be adapted into rigid in selected positions, potentially turning dry-assembled precast frames into highly dissipative and redundant structures with increased stiffness.

The freedom of selection of the joints to be adapted into rigid opens wide possibilities to the structural designer. Few seismic resisting frames may be selected in a structural arrangement, leaving the others with hinged beam-column joints for gravity load bearing only. By providing a rigid diaphragm to ensure the collaboration of the stiffer bracing frames with the gravity load bearing ones, relevant saving of material may be obtained.

The joint adaptation into rigid may be designed, as an alternative, only at selected floors, for instance the first floor or the roof. This may provide a solution to the frequent design cases in which one or few floors are subjected to a much larger gravity load, if compared with the others, due to several reasons (a different use, need of installation or circulation of heavy machines, interruption of columns, etc). If adopting hinged beam-column joints at those floors, the column size and reinforcement would not be affected by the capacity design related to the deep beams needed to sustain the load, which could lead to a remarkable reduction of the column cross-section and a general structural rationalisation. Even if geometrically regular in elevation and plan, structures with non-regular distribution of adapted joints may turn into irregular.

The joint adaptation is particularly interesting for pre-stressed concrete beams/slabs. If the horizontal members are supported on corbels and connected as hinges (i.e. with dowels), the dead loads give a simply supported moment distribution. All nodes are not then stressed by moment due to the dead loads, while those nodes adapted into rigid will be stressed by the additional live gravity loads and by the lateral loads (wind or earthquake) only. If, for instance, the live loads were approximately equal to the dead, the precast joint would be designed for a maximum moment equal to half of that of a cast-in-situ. This assumption is correct only if the beam does not tend to rotate in time at its ends due to creep effects, which may be obtained through a proper design of the pre-stressing. Fig. 1a shows the bending effects of dead loads on beams, where it is assumed that all dead loads are applied during the assemblage of the structure, and Fig. 1b shows the effects of the application of horizontal loads. The envelope at the lower side of the beams (Fig. 1c), considered also inverting the horizontal load direction, provides an almost constant positive bending moment profile along the beams, which may result in an optimal exploitation of the prestressing tendons.

From a practical point of view, the joint adaptation described above can be obtained by assembling the structure according to the following phases: (a) installation of the beam with hinged joint; (b) installation of the slab elements with hinged joints; (c) activation of beam-column mechanical reinforcement couplers; (d) filling of the construction joint.

In the framework of a highly industrialised precast concrete manufacturing [38], the elements can be transported to the construction site already provided with the dead non-structural technologic layers. In

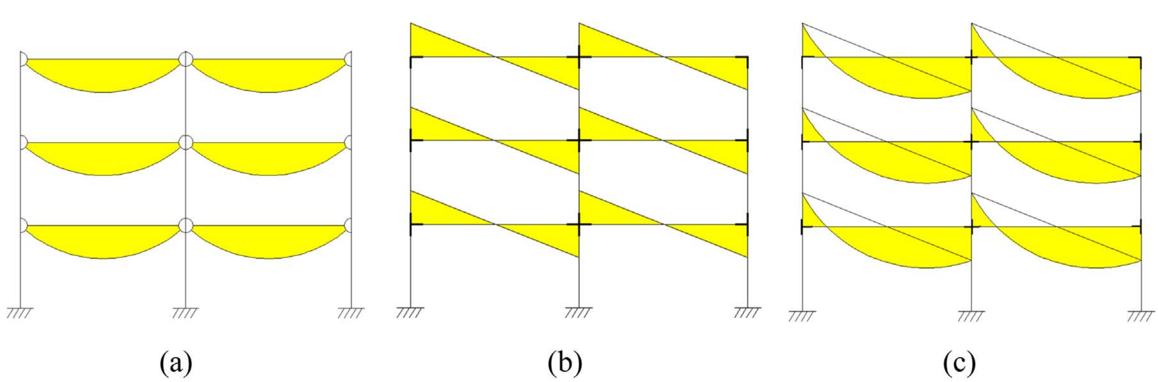

Fig. 1. Bending moment distribution along the beams: (a) dead loads, (b) horizontal loads, (c) envelope combination of both.

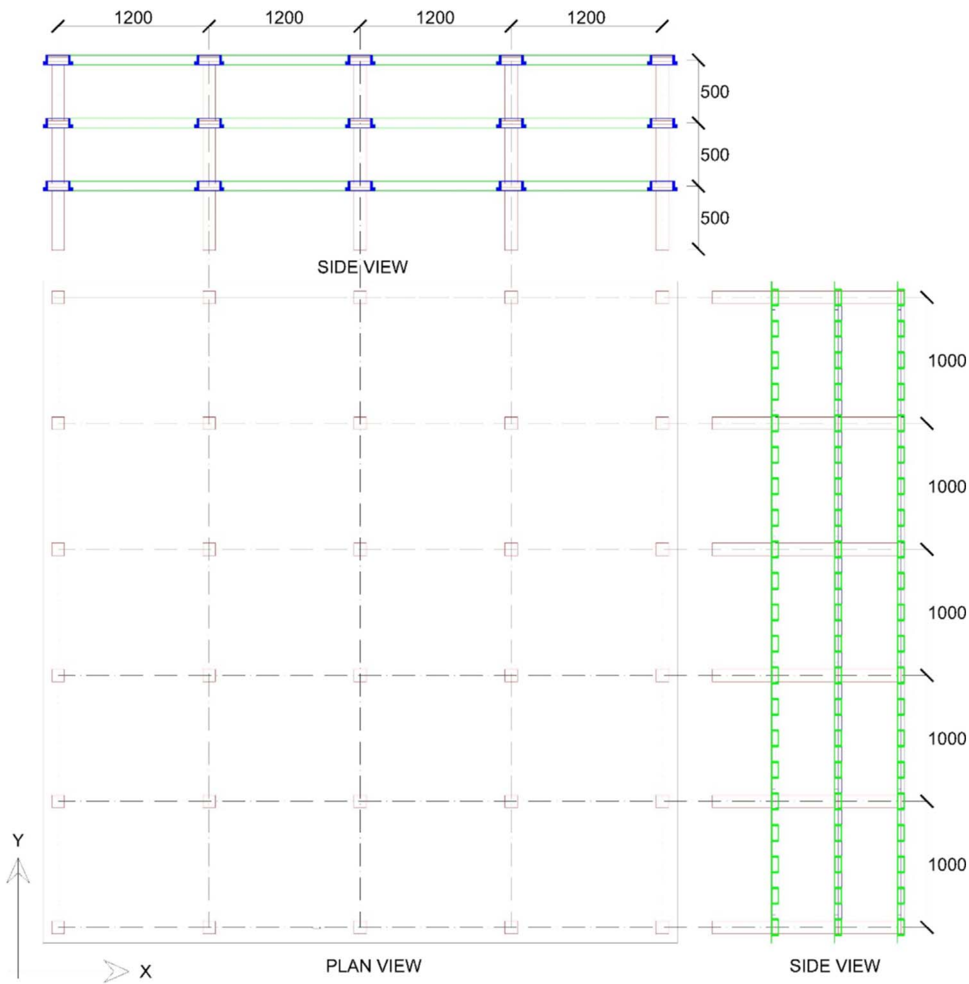

Fig. 2. Case-study building (dimensions in cm).

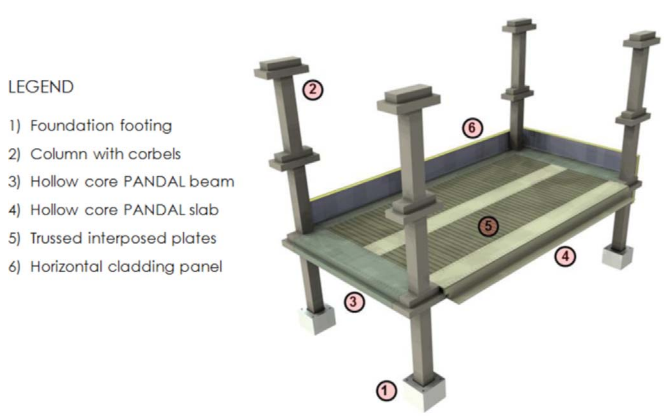

Fig. 3. Scheme of the Pandal® system (courtesy of DLC Consulting).

this case, all the dead loads will be transferred according to the simply supported static scheme. Elsewise, the dead structural loads only will be transferred according to this mechanism.

Examples of mechanical reinforcement couplers are provided in [39–42].

The viability of the above assumptions is investigated through a design case study of a multi-storey commercial building designed with modal analysis with response spectrum, and through a real application of PSAJ building subjected to pseudo-dynamic testing, whose seismic performance with different static schemes is also validated against the results of dynamic non-linear analyses performed with different models.

3. Design comparison of a case-study PSAJ building with modal dynamic analysis with response spectrum

A comparison study was performed on a case-study three-storey frame building with commercial function using the traditional design method of modal dynamic analysis with response spectrum. 3D FEM models of the building were built, where columns and beams of the frame were modelled elastically with beam elements. The building is made of a regular frame with 4 × 5 bays with 12 × 10 m span and the inter-storey height is 5 m (Fig. 2). A schematic layout of the precast system considered for this case-study is shown in Fig. 3. The monolithic square columns are provided with wide corbels to reduce the floor span. A special wide voided shallow beam allows the bay length of the floor members to be reduced and becomes part of the slab, also providing large torsional stiffness and strength. The voided floor/roof members have the same depth of the beam and of the column corbel and a special stronger member is placed along the column line for framing in the direction perpendicular to the beam. In the case-study, the floor/roof elements are installed adjacently.

Three different structural configurations were designed and compared:

(I) Precast frame with hinged beam-column connections;
(II) Precast frame with moment resisting beam-column connections activated at the roof;
(III) Precast frame with moment resisting beam-column connections activated everywhere.

The direct comparison made in the following with the cast-in-situ

Table 1
Static loads.

LOAD	kN/m^2
live	6.00
snow	1.20
dead non-structural	1.50
dead non-structural roof	1.20
wind (peak at the top)	1.05
wind (peak at the base)	0.75

equivalent frame is fictitious, due to the large spans of the case-study building, which would require the pre-stressing technology for obtaining reasonable member dimensions and service performance.

The main assumptions for the comparison were the following:

- Same gravity non-structural and wind loads and same Peak Ground Acceleration (PGA);
- Same bay, span and height dimensions of the building;
- Same member typology with variable column width or beam depth;
- External stair core(s) structurally separated from the frame (not considered);
- Light cladding panels not interacting with the frame structure (for instance metallic sandwich panels connected with low-friction sliding connections);
- Perfectly rigid diaphragm;
- Centre of the mass coincident with the centre of stiffness (no torsion);
- Beam-column connections considered as perfect hinges and, when adapted, perfectly rigid.

Concrete class C45/55 and steel grade B450C were used. The column stiffness was reduced by 50% as suggested by EC8 [27] to consider concrete cracking.

The loads applied to the structure are indicated in Table 1. The structural weight varied for each structural configuration. A relatively high live load was considered, due to possible presence of large crowds or goods vehicle circulation (corresponding to load category C5 in EC1 [43]). The snow and wind load are typical of a location of the Padana plain in Northern Italy [44]. The dead structural loads associated to the simply supported slab elements were considered equal to 2.20 kN/m^2 and were applied to the main beams. The voided beams are 2.4 m wide with variable depth. The seismic design was performed with a modal dynamic analysis with response spectrum with an ULS PGA equal to 0.25 g and a response spectrum according to EC8 [27] corresponding to sub-soil class B (α_g = 0.30 g). Since the main objective of this design phase was to compare the distribution of bending moment, the results from the modal dynamic analysis were supposed to provide valuable information, while shear distribution and storey forces would have needed to be deeper evaluated in accordance with more sophisticated design methods, as stated in [45,46]. The usual uncertainty in the definition of the vertical actions may be applied on the frames with rigid joints. However, no uncertainty was considered in the proposed design examples.

3.1. Dynamic parameters

The dynamic parameters of the three precast prototypes are reported in Table 2. The fundamental period associated to the first vibration mode in each main direction decreases with increasing structural stiffness and redundancy. The participation factor related to the

Table 2
Dynamic parameters of the three structures.

(I) PRECAST BUILDING WITH HINGED BEAM ENDS			
MODE	PERIOD [s]	PART. FACTOR X	PART. FACTOR Y
1	1.51	0.71	0.00
2	1.51	0.00	0.71
3	0.27	0.23	0.00
4	0.27	0.00	0.23
(II) PRECAST BUILDING WITH RIGID ROOF BEAM ENDS			
MODE	PERIOD [s]	PART. FACTOR X	PART. FACTOR Y
1	1.38	0.80	0.00
2	1.32	0.00	0.81
3	0.28	0.16	0.00
4	0.26	0.00	0.15
(III) PRECAST BUILDING WITH RIGID BEAM ENDS			
MODE	PERIOD [s]	PART. FACTOR X	PART. FACTOR Y
1	0.89	0.86	0.00
2	0.74	0.00	0.89
3	0.28	0.11	0.00
4	0.25	0.00	0.10

Table 3
Design highlights for the three buildings.

(I) PRECAST BUILDING WITH HINGED BEAM ENDS			
member dimensions [mm]			
column width	1000		
beam depth	600		
roof beam depth	400		
displacements[mm]			
storey	1	2	3
wind in x	2.5	8.0	14.6
wind in y	2.5	8.0	14.6
earthquake in x - ULS	35 0.7%	115 1.6%	212 1.9%
earthquake in y - ULS	35 0.7%	115 1.6%	212 1.9%
earthquake in x - DLS	14 0.3%	46 0.6%	85 0.8%
earthquake in y - DLS	14 0.3%	46 0.6%	85 0.8%
θ - wind in x	0.20	0.22	0.13
θ - wind in y	0.20	0.22	0.13
θ - earthquake in x	0.18	0.12	0.07
θ - earthquake in y	0.18	0.12	0.07
seismic storey forces [kN]			
earthquake in x - ULS	2375	4750	3156
earthquake in y - ULS	2375	4750	3156
force reduction factor		1.5	

(II) PRECAST BUILDING WITH ROOF BEAM ENDS ADAPTED INTO RIGID			
member dimensions [mm]			
column width	850		
beam depth	600		
roof beam depth	600		
displacements[mm]			
storey	1	2	3
wind in x	1.4	2.9	3.7
wind in y	0.9	1.6	2.0
earthquake in x -ULS	45 0.9%	98 1.1%	127 0.6%
earthquake in y -ULS	43 0.9%	86 0.9%	105 0.4%
earthquake in x - DLS	18 0.4%	39 0.4%	51 0.2%
earthquake in y - DLS	17 0.3%	34 0.3%	42 0.2%
θ - wind in x	0.11	0.06	0.02
θ - wind in y	0.06	0.03	0.01
θ - earthquake in x	0.23	0.08	0.02
θ - earthquake in y	0.18	0.05	0.01
seismic storey forces [kN]			
earthquake in x - ULS	2396	4792	3184
earthquake in y - ULS	2483	4965	3299
force reduction factor		1.5	

(III) PRECAST BUILDING WITH BEAM ENDS ADAPTED INTO RIGID			
member dimensions [mm]			
column width	750		
beam depth	600		
roof beam depth	600		
displacements[mm]			
storey	1	2	3
wind in x	1.1	2.3	2.9
wind in y	0.7	1.3	1.5
earthquake in x -ULS	40 0.8%	88 1.0%	114 0.5%
earthquake in y -ULS	37 0.7%	74 0.7%	91 0.3%
earthquake in x - DLS	16 0.3%	35 0.4%	45 0.2%
earthquake in y - DLS	15 0.3%	30 0.3%	36 0.1%
θ - wind in x	0.09	0.05	0.01
θ - wind in y	0.06	0.02	0.00
θ - earthquake in x	0.27	0.09	0.08
θ - earthquake in y	0.21	0.06	0.04
seismic storey forces [kN]			
earthquake in x - ULS	1818	3635	2416
earthquake in y - ULS	2169	4338	2883
force reduction factor		3.0	

first mode, on the other hand, is increasing, providing a lower influence of higher modes. The period of higher modes does not considerably change with the redundancy.

3.2. Design highlights

The design highlights are collected in Table 3. The storey forces were calculated according to the chosen design methodology. A graphic description of the moment distribution on the critical members is given in Fig. 4 for the beams and in Fig. 5 for the columns. Since the column cross-section is symmetric, the envelope of bending moments is drawn on one side only. Even if introduced in the EC8 [27] for seismic loads, the inter-storey drift sensitivity coefficient θ was also evaluated under wind lateral load, to provide information about the tendency to the rise of second order effects also for the wind load combination.

The horizontal members of the building with hinged nodes were designed for gravity loads only, since they were not part of the lateral load resisting system of the building. The building was remarkably flexible, with first period equal to 1.51 s. The seismic demand was reduced, since a smaller acceleration with respect to that of the ground was obtained. The critical design verification was the inter-storey drift sensitivity coefficient θ at ULS, rather than the deformability at DLS or the strength of the base of the column. Such coefficient gained importance also in the wind load case. The cross-section of the columns was therefore the key parameter to control the stiffness of the building. The indication of EC8 [27] suggesting adopting a minimum width dimension equal to a tenth of the shear length, given θ is larger than 0.10, was not respected (it would have led to 1.5 m of width). The force reduction factor q was taken equal to 1.5 (elastic behaviour) to keep the value of θ lower than 0.3. As a matter of fact, given the value of the inter-storey drift sensitivity coefficient θ is directly proportional to the inter-storey displacement d_r by definition, and d_r needs to be multiplied by the force reduction factor q, the value of θ is directly proportional to the value of q.

For the building with clamped roof, the joints of roof beams and floors (only those elements in correspondence of the columns) were in this case turned into rigid, forming a portal frame as tall as the whole structure in two directions with the columns. The horizontal members

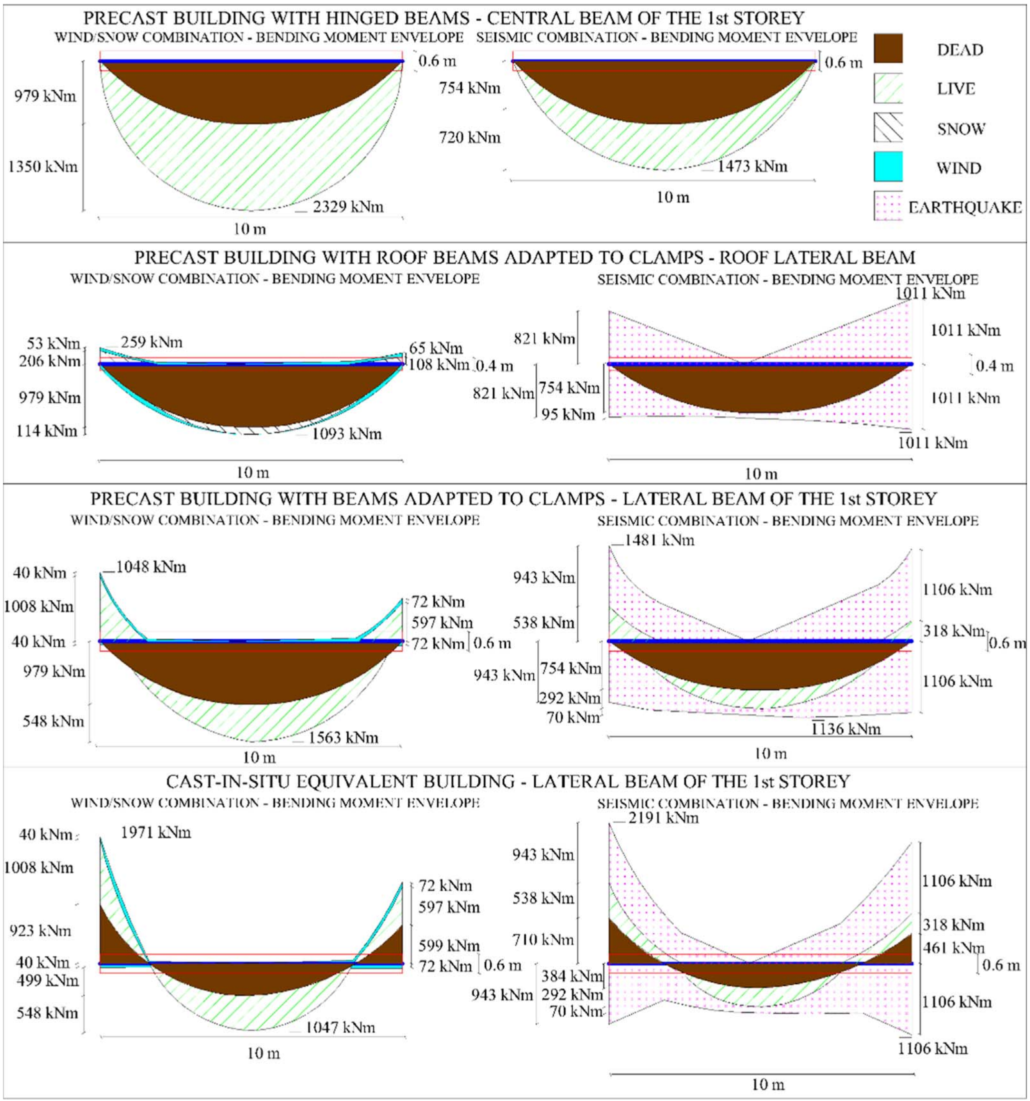

Fig. 4. Bending moment envelope distribution for beams.

at the lower stories were still not involved in the lateral load resisting system.

The seismic design of the building was again determined by the θ factor, while the strength of members and the DLS limitations were widely fulfilled. The height of the roof slab was increased with respect to the previous case due to the need of both higher strength and global stiffness. The cross-section of the column was again the key parameter in the design process. The indication of EC8 on the minimum width of the column would have led to 0.75 m, less than the adopted.

In the case of the fully moment-resisting frame, all the beams were involved into the lateral load resisting system. The key parameters for the design were the axial-flexural strength at the base of the columns, the application of the capacity design in its strong column-weak beam corollary and, again, the fulfilment of the θ factor requirements. Thus, all the required verifications played a crucial role in the design, which was more balanced. To be noted that only for this latter static scheme the θ factor associated to the wind action was lower than 0.1 at all stories.

Resuming, the comparative design shows that:

- The stiffness remarkably increases moving from the fully hinged through the clamped roof to the fully moment-resisting frame;
- Beams and floor members, when hinged, are designed only for gravity loads and, as a matter of fact, the strong column - weak beam criterion is neglected;
- The precast beams, initially simply supported and afterwards connected through rigid joints, are more rationally exploited, since in the seismic load combination the envelope of bending moments in critical zone (the edges) is such that the positive and negative bending moments are very similar, differently from the cast-in-situ equivalent beam;
- For frames with clamped storeys other than the roof, the reduced bending moment of the precast clamped beam with respect to a cast-in-situ equivalent can lead to smaller column cross-sections;
- The bending moment distribution in columns is enhanced passing from the hinged beams scheme to the roof clamped to the fully clamped, also with relevant reduction of the base action, which determines the design of the foundations.

4. Non-linear dynamic behaviour of a real PSAJ building

4.1. Prototype

The seismic performance of a PSAJ building was experimentally studied in the framework of the SAFECAST research project [47] through pseudo-dynamic testing of a full-scale prototype structure at the European Laboratory of Structural Assessment (ELSA) of the Joint Research Centre (JRC) of the European Commission. DLC Consulting of

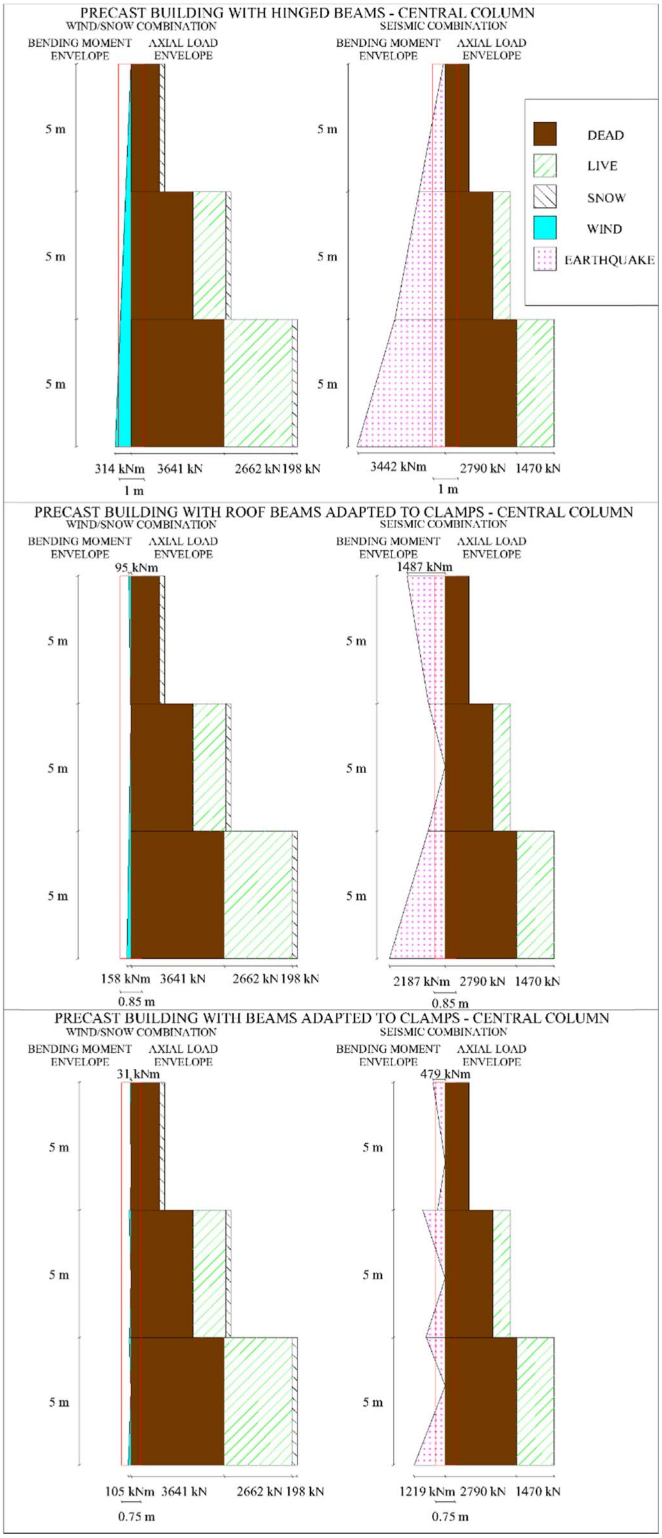

Fig. 5. Bending moment envelope distribution for columns.

Milan, technical partner of the consortium of the SAFECAST project, carried out the design of the prototype. The building was a regular three stories frame for office use, made with two 7 m bays in each direction and inter-storey height of 3.4-3.2-3.2 m. It is the world largest precast building built for research purposes up to the present. More details about the structure can be found in [48–50], together with a detailed report of the results of the experimental campaign.

A schematic layout of the precast system used to build the prototype is shown in Fig. 3. The technology used was the same of that of the case-study building introduced in the previous paragraph, with the only difference being the installation of double-T floor elements at the 2nd storey only. A picture of the prototype is shown in Fig. 6.

Fig. 6. Full scale prototype of PSAJ building tested at the ELSA/JRC laboratory of Ispra (Italy). The walls are de-coupled from the frame structure in the considered tests.

The peculiar geometry of the beam-column joint is described in Fig. 7. Fig. 8 shows the monolithic columns with large corbels assembled on pocket precast foundations tied to the strong floor and the positioning of a beam on top of the corbels. The beam, after being positioned on top of the column corbels, was connected with dowels to get the hinged configuration. The dowels were in this project made by d40 steel bars enlarged by 60 mm long d52 cylindric tubes made of S275JR steel. They were welded to the bars in correspondence of the corbel-beam joint (Fig. 9a). Such a large diameter of the dowel was designed to sustain the large load needed for a rigid diaphragm effect in the test condition with bracing walls, which is not treated in the present paper (see [28,48–50] for further information). After the installation of the beam, each dowel hole was filled with high-strength expansive mortar.

After the slabs were installed, the joint was adapted into rigid by activating the rebar couplers. They were made with a special mechanical device named Kaptor® which couples the longitudinal reinforcement inserted into the column and into the beam.

Fig. 10a shows the coupler assembly. Two normal rebars of steel grade B450C are provided with an upset enlarged end, which is mechanically fixed to a strong steel plate. One plate is cast into the column and another one into the beam. A high strength bolt inserted into the beam plate and screwed in to the beam plate activates the coupling. The joint is then filled with high strength expansive mortar. The connection device provides an elastic behaviour up to the failure of the connected reinforcement and ensures a zone of energy dissipation (critical zone) that makes the node ductile. A picture of the device after a tensile test is shown in Fig. 10b. More details about the coupler and about its structural behaviour can be found in [41] with reference to a similar device used for the column-foundation connection. In the prototype, two d25 rebars were coupled by a d30 bolt of steel grade 12.9. A similar typology of connection based on welding of the rebars instead of upsetting was installed at the 2nd floor of the prototype building.

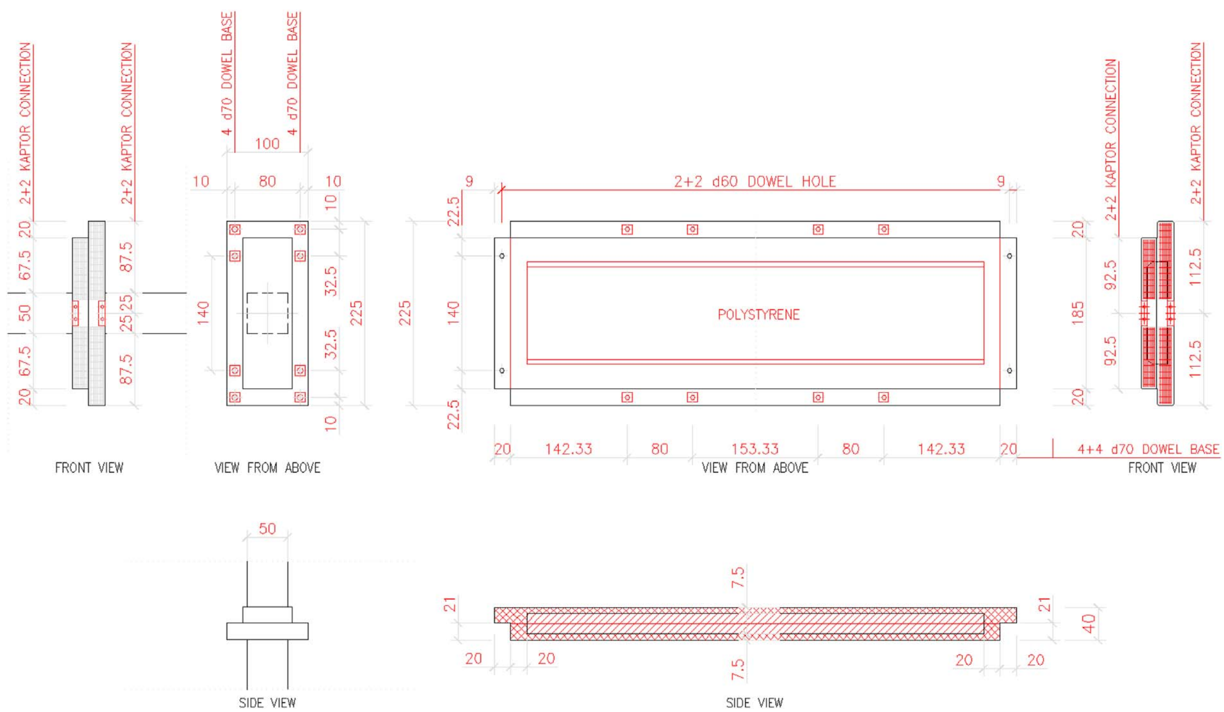

Fig. 7. Technical drawings of beam-column joint (dimensions in cm).

(a)　(b)

Fig. 8. Full-scale prototype: (a) monolithic columns with cross-shaped corbel for the support of the shallow hollow core beam and floor members, (b) beam in phase of assemblage.

Fig. 11a shows the detail of a beam edge, with vertical holes left for the insertion of the dowels positioned at the sides and the coupling connection plates positioned at the centre, with horizontal holes left for the insertion of the high-strength steel bolts (Fig. 11b) to be screwed into the beam plate (Fig. 12).

Three frame configurations, corresponding to the frame with hinged nodes, with the roof beams only adapted into rigid and fully moment-resisting were tested within one unique specimen, by progressively adapting the joints into rigid by activating the mechanical coupling devices.

4.2. Numerical models

The above-described structures were numerically modelled, and dynamic non-linear analyses were used as blind predictions of the experimental results, without any a posteriori calibration of the models. The aim was to highlight the differences of the theoretical seismic performance of the structure as it would be simulated in a sophisticated design framework in comparison with the real behaviour.

All members were modelled with beam elements. Columns and beams were modelled with two different non-linear techniques: (a) fibre-based distributed plasticity and (b) section-based distributed plasticity. The non-linear models based on fibre distributed plasticity were built in MidasGen environment [51]. A Mander model [52] was used for both confined and unconfined C45/55 concrete. A Menegotto-Pinto model [53] was used for the B450C mild steel reinforcement. The structural cross-sections were modelled with 30 ÷ 40 concrete fibres and one fibre per reinforcing bar. Only the reinforcement coupled by the mechanical devices was considered in modelling the beams. The non-linear models based on sectional distributed plasticity were built in Straus7 environment [54], which provides an automatically distributed plasticity through Gauss-Lobatto points based on the definition of a sectional moment-curvature diagram for an assigned axial load. The diagrams were separately evaluated though sectional equilibrium using a Sargin model [55] for the unconfined concrete, a modified Sargin model with constant post-peak stress up to the ultimate strain evaluated according to Model Code 2010 [56] for the confined concrete, and a bi-linear elastic-hardening model for the mild steel. The Takeda hysteresis

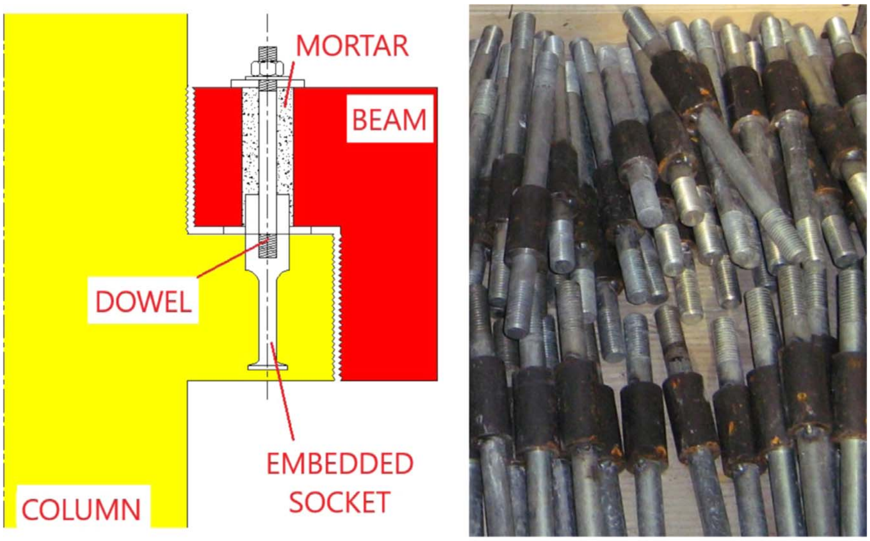

(a) (b)

Fig. 9. Enlarged dowel used for beam-column hinged connection: (a) schematic view of the joint, (b) dowels prior to installation.

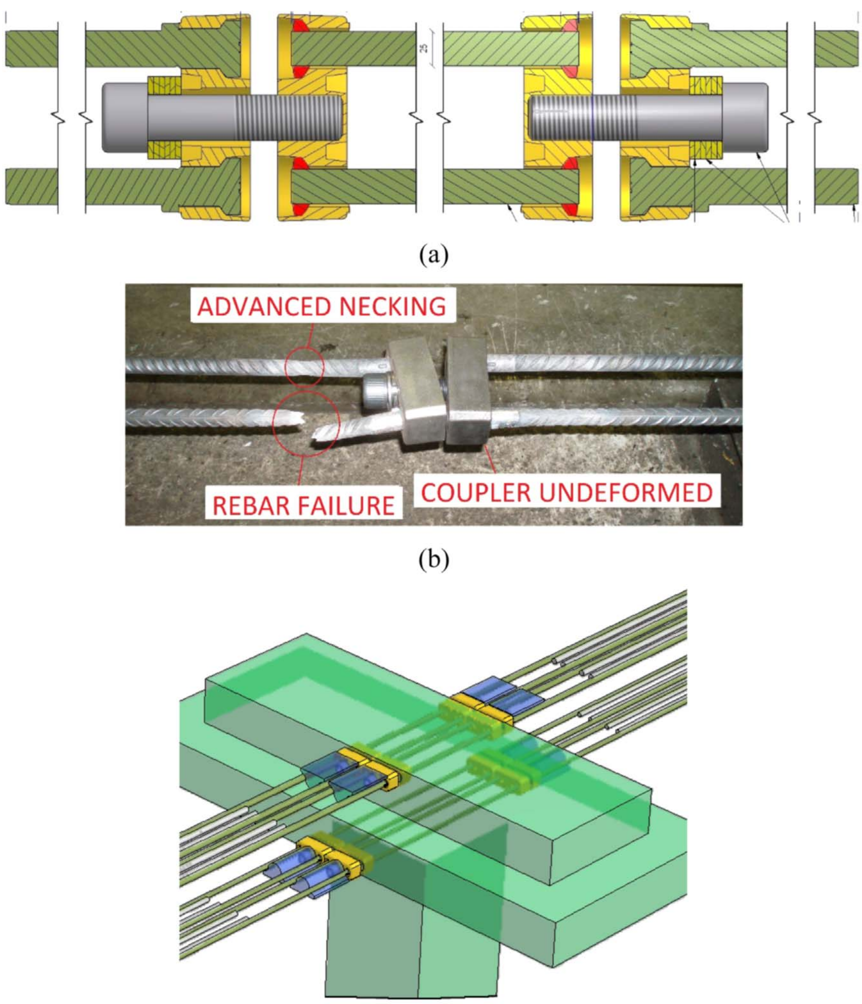

(a) (b) (c)

Fig. 10. Mechanical coupler used for beam-column rigid connection: (a) schematic view, (b) picture at the end of a tensile test, (c) installation in a roof joint.

model [57] was attributed. Nominal material strength properties were used in both the typologies of models. The elements had a length lower than the minimum dimension of the member cross-section. The floor masses (212.6-196.2-158.0t for the 1st-2nd-3rd storey) used as an input of the dynamic testing (see [58] for information about the implementation of the technique) were concentrated to the joint nodes. They included also part of the design live load of the structure, being it an office building. The real axial load acting on the structure during the

(a) (b)

Fig. 11. Detail views of one beam end: (a) rough surfaces for better interlock, innovative mechanical connections placed in correspondence of the column and holes for the dowel connection in correspondence of the rib, (b) coupling bolts of the mechanical connections.

Fig. 12. Activation of the mechanical beam-column connections by screwing of the bolts.

Table 4
Dynamic parameters of the PSAJ building prototypes.

		Frequency [Hz]	Period [s]	Participation factor [%]
Hinged beams	Mode 1	0.59	1.69	72.9
	Mode 2	4.27	0.23	23.2
Roof beams adapted	Mode 1	0.95	1.05	82.5
	Mode 2	4.75	0.21	14.8
All beams adapted	Mode 1	2.12	0.47	88.7
	Mode 2	6.51	0.15	9.7

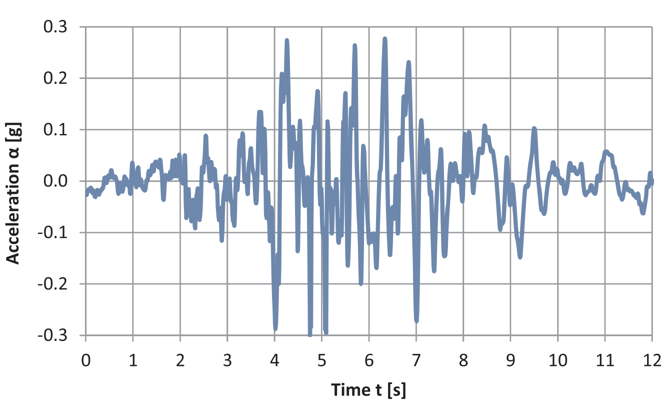

Fig. 13. Modified Tolmezzo accelerogram.

tests only included the structural self-weight (about 2/3 of the input masses). Thus, point axial loads were assigned at each beam-column node to model the real axial load acting during the tests. The base pocket foundation was modelled as a perfectly rigid connection (see [59] for experimental evidence), as well as the moment-resisting adapted beam-column joints. The floor/roof diaphragm was considered rigid. This assumption was proved to be reasonable after the test results, as commented in [50]. A Rayleigh-type viscous damping was assigned with a 2% damping ratio imposed to the natural frequencies corresponding to the first two main vibration modes of the structure evaluated considering a halved elastic stiffness of the members included in the lateral load resisting system. This value of damping is lower than the traditional 5% suggested by EC8 [27]. This is due to the fact that the main source of additional damping in a R.C. building is correlated to the damage of non-structural elements which, however, were not installed in the experimental mockup. The natural vibration frequencies associated to the first two relevant modes are reported in Table 4. The trend of periods and participation factors follows the one found in the case-study previously described.

4.3. Numerical and experimental results

The Tolmezzo earthquake (Fig. 13), with a duration of 12 s, modified to fit the response spectrum given by EC8 [27] was applied to the prototype in all its structural configurations, scaled at a PGA equal to 0.30 g, corresponding to the structure design PGA at ULS. Both experimental and numerical results of the frame configuration with hinged beam-column nodes are plotted in Fig. 14. A low elastic stiffness was reported, and the effect of higher modes was predominant in the response, as it can be observed by the confused peaks of the base shear-displacement plots, due to counter-acting storey displacements. The high deformability led to large displacements. The comparison between numerical and experimental vibratory curves shows that the hysteretic trend was correctly caught, even if remarkable discrepancies occurred after about 6 s, to which corresponds an apparent gain of stiffness or damping of the structure which is not caught by any of the models, which predicted a quasi-free-vibration response with much larger amplitude cycles than those obtained in the test. This discrepancy was also observed in [60]. A possible interpretation of this discrepancy is related to the geometrically non-linear behaviour of the joint at large relative rotation because of the angle contacts (similar findings were observed in another full-scale test of a precast structure [61]) (Fig. 15).

The case with clamped roof, the results of which are collected in Fig. 16, still showed large displacements comparable with those of the previous structural configuration. Nevertheless, the elastic stiffness was higher, and the effect of higher modes was reduced, providing a more regular response with lower storey forces. The results from both numerical models provided a good estimation of the response.

The activation of the connections at all nodes furthermore improved the seismic behaviour, although forces were larger. The results are collected in Fig. 17. Some scatter is found in the comparison between

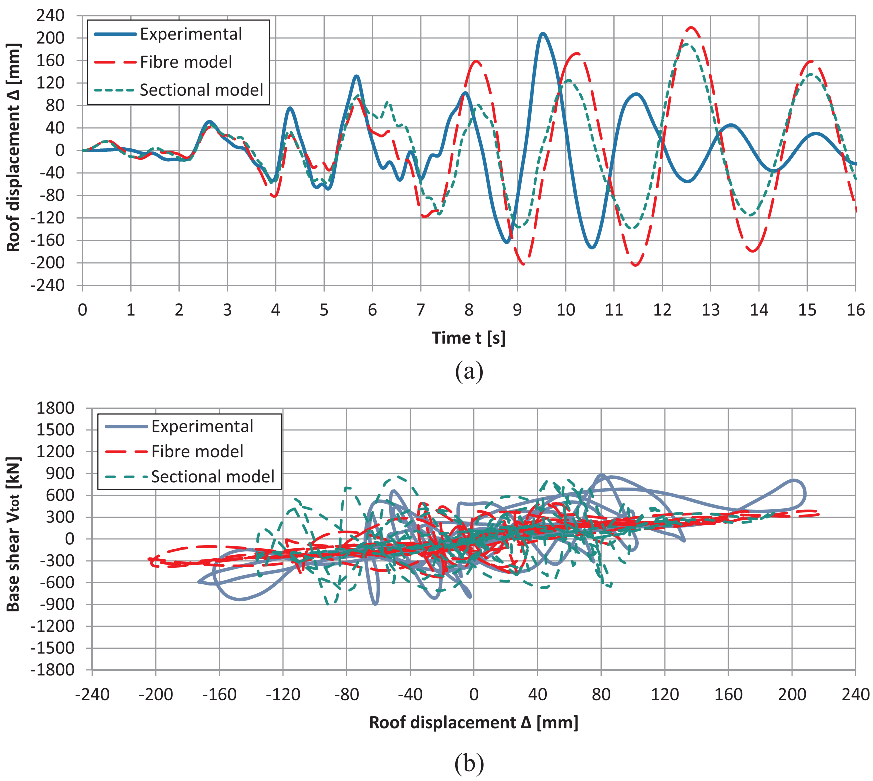

Fig. 14. Structure with hinged beam-column connections: (a) roof displacement time histories, (b) base shear vs roof displacement.

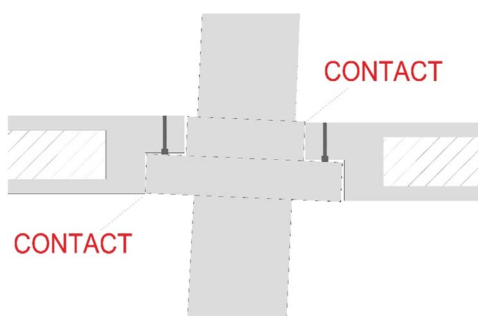

Fig. 15. Kinematics of the beam-column joint with dowel connection at large rotation and gap closing as a possible explanation of stiffness gain.

experimental and numerical results, particularly after 5 s, with larger experimental displacements. The experimental base shear vs top displacement plot shows a pinching tendency around null displacement which was not caught by the numerical models.

A technological reason might explain this scatter: while dismantling the structure, which occurred reversing the assemblage process through the de-activation of the mechanical connections unscrewing the bolts, it was observed that several nodes distributed through the stories were not satisfactorily filled with the mortar [62].

The measurements taken by the laboratory staff on few selected nodes [50] confirmed that some of them acted as perfectly rigid, while others acted as semi-rigid connections, which was due to the arrest of the mortar flow before filling the lower area of some nodes. Fig. 18 shows the difference between correctly and poorly filled nodes through pictures taken during dismantling. This suggests that the filling operation shall be more carefully designed and detailed, for instance with the introduction of gutters within the corbel and larger interface distances to avoid the grouting flow to arrest.

In this case only, the numerical predictions of fibre and sectional models showed relevant differences between them, which might have been due to the continuous change of axial load in the columns occurring during the seismic excitation, due to the framing with the beams. As a matter of fact, this change is only caught by the fibre-based model, while the assigned moment vs curvature diagram for the sectional-based model is only referred to a single axial load and is not updated through the analysis.

The efficiency of the rigid-adapted connection, where the filling was correctly executed, was accompanied by the development of beam crack patterns which suggest a pull-out mechanism (Fig. 19), together with spalling of the concrete surrounding the rebars within the plastic length which developed. In order to leave the rebars entering the plastic field avoiding concrete spalling and cracking, the adoption of debonding sleeves for the expected length of plastic hinge is proposed, which would also avoid problems of early juxtaposition of the longitudinal pre-stressing tendons with the ductile rebars.

The final cyclic test [48–50] pushed the structure up to an interstorey drift of 6% without showing tendencies to failure, after which the test was stopped for the attainment of the maximum stroke of the jacks, demonstrating however the large ductility properties of the moment-resisting adapted frame.

5. Conclusions

An innovative solution for dry-assembled precast structures is proposed, where the traditional beam-column hinged joints can be adapted into rigid in desired locations. The potential benefits of precast structures with adaptable joints with respect to both traditional dry-assembled precast frames and cast-in-situ or wet-assembled precast frames are discussed. In particular, the activation of the mechanical connections adapting the joint from hinged into rigid is performed after the dead loads are applied, allowing the end joints not to be stressed in flexure by dead loads. The bending moment envelope of the horizontal members allows a remarkable reduction of the maximum values and an optimal exploitation of the pre-stressing reinforcement. The freedom of selection of the joints to be adapted provides the structural designer with a viable range of options for a more versatile design, offering solutions to complex structural design issues.

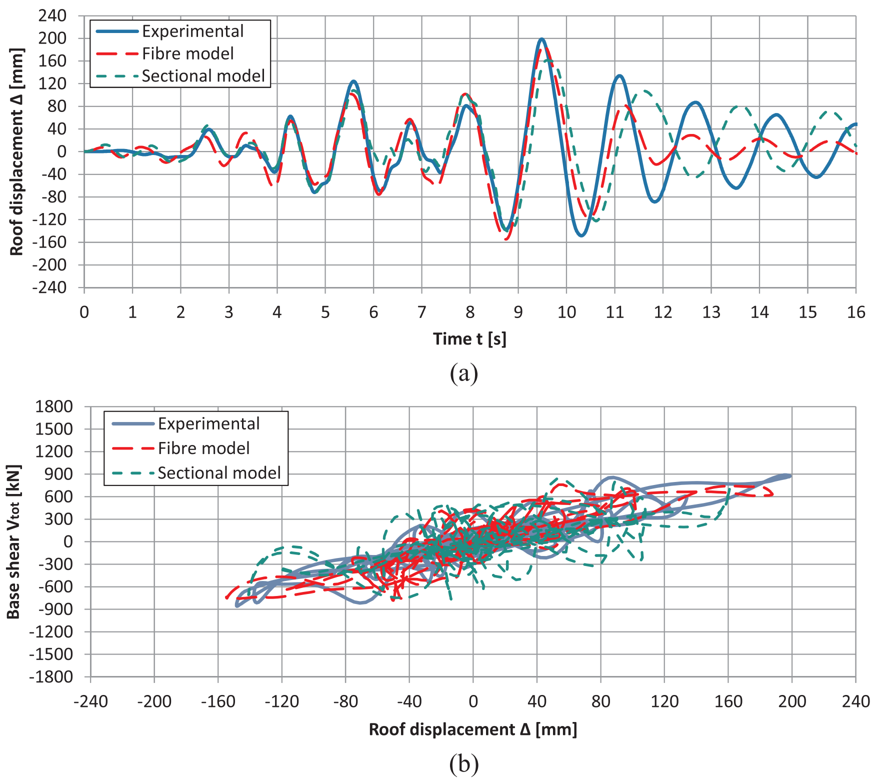

Fig. 16. Structure with beam-column connections adapted into rigid only at the roof: (a) roof displacement time histories, (b) base shear vs roof displacement.

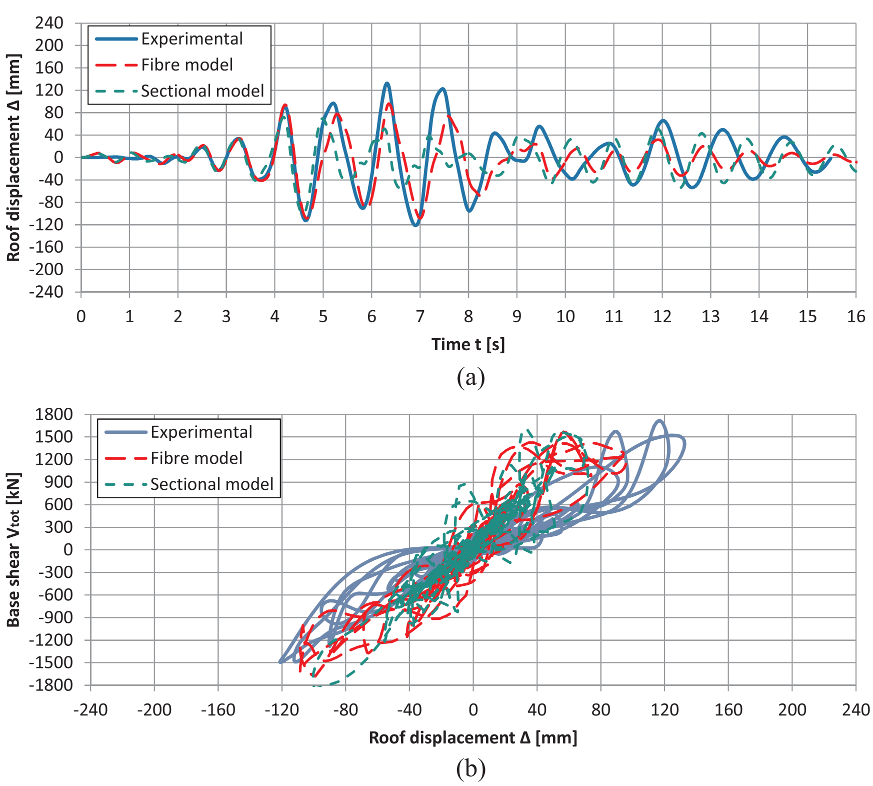

Fig. 17. Moment-resisting frame: (a) roof displacement time histories, (b) base shear vs roof displacement.

The seismic design of a case-study structure with three different static schemes shows how the structure can be optimised with the different configurations, limiting the large flexibility of traditional precast structures and rationalising the structural members. An experimental campaign concerning pseudo-dynamic testing on a full-scale prototype of precast structure with adaptable joints with static schemes ranging from cantilever column type to fully moment-resisting frame showed the seismic performance of the proposed solutions and the viability of the technique used for the semi-dry joint adaptation. The blind predictions of non-linear dynamic analyses performed with fibre- and sectional-based models provided a good estimation of maximum displacements, base shear forces and dynamic trends. However, both numerical models over-estimated the post-peak vibration trend for the structure with hinged beam-column connections, probably due to the

(a)
(b)

Fig. 18. Joints adapted into rigid after beam removal: (a) correctly filled joint, (b) node filled with mortar at the upper part only. The lateral dowels are clearly visible.

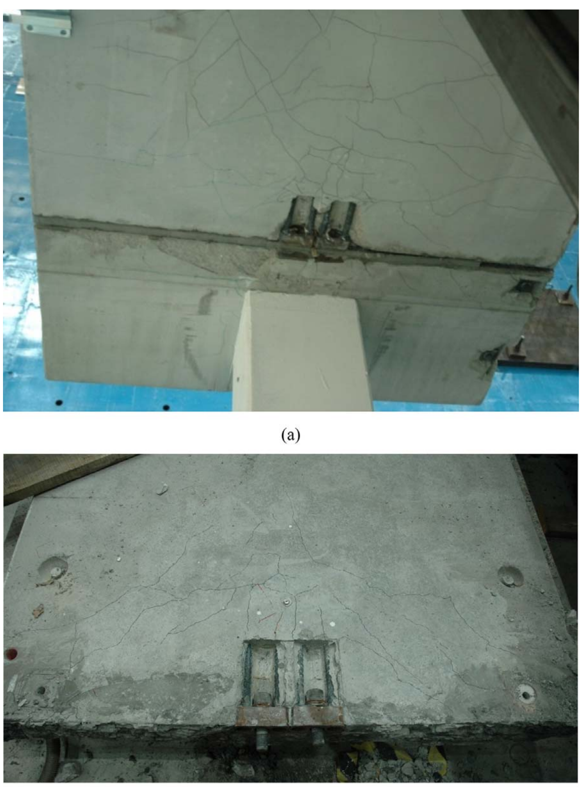
(a)
(b)

Fig. 19. Typical pull-out crack pattern of a beam after the end of the tests with spalled concrete around the mechanical connections due to their plastic elongation: (a) lower side, (b) upper side after dismantling.

non-linear behaviour of the hinged joints at large rotations. Furthermore, both numerical models under-estimated the amplitude of the vibrations in the case of fully moment-resisting frame structure, which was due to the only partial filling of some nodes with the mortar. Improved technological solutions are proposed to avoid this issue. The fibre-based model, being able to update the sectional moment-curvature diagram with the continuous change of axial load in the columns during seismic excitation, provides a better response prediction for structures with adapted joints.

The results show that dry-assembled precast structures with adaptable joints can attain lower seismic drifts with respect to traditional precast structures, potentially rationalising the structural elements while enhancing the global redundancy.

Acknowledgments

Antonella Colombo from Assobeton, prof. Giandomenico Toniolo, prof. Fabio Biondini and Marco Lamperti from Politecnico di Milano, among other partners, are gratefully acknowledged for the common work carried out within the SAFECAST research project (FP7-SME-2007-2; Grant agreement n. 218417/2009). The team of the Experimental Laboratory of Structural Assessment of the Joint Research Centre of the European Commission in Ispra (Italy) is also acknowledged for the execution of the pseudo-dynamic tests on the full-scale prototype. Pizzarotti Prefabbricati company is acknowledged for the production, erection and dismantling of the prototype. Diego Dal Lago from DLC Consulting of Milan is acknowledged for the technical drawings of the precast system and its connections.

References

[1] Mandelli Contegni M, Palermo A, Toniolo G. Strutture prefabbricate: schedario di edifici prefabbricati in cemento armato. Civil Protection Department, ReLUIS and Assobeton; 2008. [in Italian].
[2] Bonfanti C, Carabellese A, Toniolo G. Strutture prefabbricate: catalogo delle tipologie esistenti. Italian Civil Protection Department, ReLUIS and Assobeton; 2008. [in Italian].
[3] Biondini F, Toniolo G. Probabilistic calibration and experimental validation of the seismic design criteria for one-storey concrete frames. J Earthq Eng 2008;13:426–62.
[4] Dal Lago B. Experimental and numerical assessment of the service behaviour of an innovative long-span precast roof element. Int J Conc Struct Mater 2017;11(2):261–73.
[5] Ferrara L, Mola E, Negro P. Pseudodynamic and cyclic testing of full scale prototypes of precast R/C one storey buildings. 1st ECEES; 2006, Geneva, Switzerland.
[6] Fischinger M, Kramar M, Isaković T. Cyclic response of slender RC columns typical of precast buildings. Bull Earthq Eng 2008;6(3):519–34.
[7] Biondini F, Toniolo G, Tsionis G. Capacity design and seismic performance of multi-storey precast structures. Eur J Environ Civil Eng 2010;14(1):11–28.
[8] Ferrara L, Colombo A, Negro P, Toniolo G. Precast vs. cast-in-situ RC industrial buildings under earthquake loadings: an assessment via pseudo-dynamic tests. 13th WCEE; 2004, Vancouver, Canada.
[9] Ferrara L, Mola E, Negro P. Design of earthquake resistant precast structures: lessons derived from a co-normative research project. 4th International Conference on the conceptual approach to structural design; 2007, Venezia, Italy.
[10] Bournas DA, Negro P, Molina FJ. The importance of connections in seismic regions: full-scale testing of a 3-storey precast concrete building. Exp Res Earthq Eng Ser Geotech Geol Earthq Eng 2015;35:387–403.
[11] Toniolo G, Colombo A. Precast concrete structures: the lesson learnt from L'Aquila earthquake. Struct Conc 2012;13(2):73–83.
[12] Biondini F, Dal Lago B, Toniolo G. Role of wall panel connections on the seismic performance of precast structures. Bull Earthq Eng 2013;11(4):1061–81.
[13] Magliulo G, Ercolino M, Manfredi G. Influence of cladding panels on the first period of one-story precast buildings. Bull Earthq Eng 2014;13(5):1531–55.
[14] Babič A, Dolšek M. Seismic fragility functions of industrial precast building classes. Eng Struct 2016;118:357–70.
[15] Belleri A, Torquati M, Marini A, Riva P. Horizontal cladding panels: in-plane seismic performance in precast concrete buildings. Bull Earthq Eng 2016;14(4):1103–29.
[16] Bournas D, Negro P, Taucer F. Performance of industrial buildings during the Emilia earthquakes in Northern Italy and recommendations for their strengthening. Bull Earthq Eng 2013;12(5):2383–404.
[17] Magliulo G, Ercolino M, Petrone C, Coppola O, Manfredi G. Emilia earthquake: the seismic performance of precast RC buildings. Earthq Spectra 2014;30(2):891–912.
[18] Belleri A, Brunesi E, Nascimbene R, Pagani M, Riva P. Seismic performance of precast industrial facilities following major earthquakes in the Italian territory. J Perf Constr Facil 2015;29(5):04014135.
[19] Dal Lago B, Biondini F, Toniolo G, Lamperti Tornaghi M. Experimental investigation on the influence of silicone sealant on the seismic behaviour of precast façades. Bull Earthq Eng 2016;15(4):1771–87.
[20] Zoubek B, Fischinger M, Isaković T. Cyclic response of hammer-head strap cladding-to-structure connections used in RC precast buildings. Eng Struct 2016;119:135–48.
[21] Zoubek B, Fischinger M, Isaković T. Seismic response of short restrainers used to protect cladding panels in RC precast buildings. J Vib Control 2016. http://dx.doi.org/10.1177/1077546316659780.
[22] Toniolo G, Dal Lago B. Conceptual design and full-scale experimentation of cladding panel connection systems of precast buildings. Earthq Eng Struct Dyn 2017. http://dx.doi.org/10.1002/eqe.2918.
[23] Negro P, Lamperti Tornaghi M. Seismic response of precast structures with vertical

cladding panels: the SAFECLADDING experimental campaign. Eng Struct 2017;132:205–28.
[24] Dal Lago B, Biondini F, Toniolo G. Experimental investigation on steel W-shaped folded plate dissipative connectors for precast cladding panels. J Earthq Eng 2017. http://dx.doi.org/10.1080/13632469.2016.1264333.
[25] Dal Lago B, Biondini F, Toniolo G. Friction-based dissipative devices for precast concrete panels. Eng Struct 2017;147:356–71.
[26] Dal Lago B, Ferrara L Efficiency of mechanical floor connections on the diaphragm action of precast concrete floor/roof decks. 14th ISSE 2016, Beijing, China;1:469-476.
[27] EN 1998-1. Eurocode 8: design of structures for earthquake resistance. Part 1: general rules, seismic actions and rules for buildings. Brussels: European Committee for Standardization; 2004.
[28] Dal Lago B, Muhaxheri M, Ferrara L. Numerical and experimental analysis of an innovative lightweight precast concrete wall. Eng Struct 2017;137:204–22.
[29] Valente M. Improving the seismic performance of precast buildings using dissipative devices. 2nd ICRMCE, Solo, Indonesia;54:795-804; 2013.
[30] Belleri A, Torquati M, Riva P, Nascimbene R. Vulnerability assessment and retrofit solutions of precast industrial structures. Earth Struct 2015;8(3):801–20.
[31] Sorace S, Terenzi G. Existing prefab R/C industrial buildings: seismic assessment and supplemental damping-based retrofit. Soil Dyn Earthq Eng 2017;94:193–203.
[32] Martinelli P, Mulas G. An innovative passive control technique for industrial precast frames. Eng Struct 2010;32:1123–32.
[33] Belleri A, Marini A, Riva P, Nascimbene R. Dissipative and re-centring devices for portal-frame precast structures. Eng Struct 2017;150:736–45.
[34] Yuksel E, Karadoğan F, Bal E, Ilki A, Bal A, Inci P. Seismic behavior of two exterior beam-column connections made of normal-strength concrete developed for precast construction. Eng Struct 2015;99:157–72.
[35] Wiebe L, Christopoulos C Controlled rocking systems for enhanced seismic resilience: State of the art. IC-SDCI 2014, Shanghai, China;1:496-503.
[36] Priestley MJN, Sritharan S, Conley JR, Pampanin S. Preliminary results and conclusions from the PRESSS five-story precast concrete test building. PCI J 1999;44(6):42–67. [Special Report].
[37] Dal Lago B, Dal Lago A Precast structures with adaptable restraints. 15th WCEE 2012, Lisbon, Portugal; Paper No. 2305.
[38] Dal Lago B, Dal Lago A, Franceschelli F. Innovation for smart industrial housing. Conc Plant Int 2015;2:298–300.
[39] Englekirk RE. Development and testing of a ductile connector for assembling precast concrete beams and columns. PCI J 1995;2:36–51.
[40] Chang B, Hutchinson TC, Wang X, Englekirk RE. Experimental seismic performance of beam-column subassemblies using ductile embeds. ASCE J Struct Eng 2013;139:1555–66.
[41] Dal Lago B, Toniolo G, Lamperti Tornaghi M. Influence of different mechanical column-foundation connection devices on the seismic behaviour of precast structures. Bull Earthq Eng 2016;14(12):3485–508.
[42] Camnasio E. Bolted column connection for seismic applications. BFT Int 2017;83(8):36–43.
[43] EN 1991-1. Eurocode 1: Actions on Structures. Part 1: General Actions. Brussels: European Committee for Standardization; 2004.
[44] NTC:2008. Nuove norme tecniche delle costruzioni (NTC). Italian Ministry of Infrastructures; 2008.
[45] Rejec K, Isaković T, Fischinger M. Seismic shear force magnification in RC cantilever structural walls, designed according to Eurocode 8. Bull Earthq Eng 2012;10:567–86.
[46] Negro P, Toniolo G. Design guidelines for connections of precast structures under the seismic action. Luxembourg: Publication Office of the European Union; 2012.
[47] Toniolo G SAFECAST project: European research on seismic behaviour of the connections of precast structures. 15th WCEE 2012, Lisbon, Portugal; Paper No.1389.
[48] Bournas D, Negro P, Molina FJ, Viaccoz B, Magonette G. Pseudodynamic testing of the safecast 3-storey precast concrete building. Luxembourg: JRC Technical Report EUR 25496 EN. Publications Office of the European Union; 2012.
[49] Negro P, Bournas DA, Molina FJ. Pseudodynamic Tests on a full-scale 3-storey precast concrete building: global response. Eng Struct 2013;57:594–608.
[50] Bournas DA, Negro P, Molina FJ. Pseudodynamic Tests on a full-scale 3-storey precast concrete building: behaviour of the mechanical connections and floor diaphragms. Eng Struct 2013;57:609–27.
[51] MIDAS Information Technology. MIDAS/Gen-General structure design system. MIDAS/Gen Version 8.25 Analysis and Design Manual; 2013.
[52] Mander J, Priestley M, Park R. Theoretical stress-strain model for confined concrete. J Struct Eng 1988;114(8).
[53] Menegotto M, Pinto PE . Method of analysis of cyclically loaded RC plane frames including changes in geometry and non-elastic behavior of elements under normal force and bending. Report IABSE 13; 1973.
[54] G+D Computing. Using Strand7 (Straus7) - Introduction to the Strand7 finite element analysis system. ed. 3 Strand7 Pty Limited; 2010.
[55] Sargin M, Handa VK. A general formulation for the stress-strain properties of concrete. Solid Mech Div 1969;3:1–27.
[56] *fib*. Model code for concrete structures. Fédération Internationale du Béton / International Federation for Structural Concrete 2010, Lausanne, Switzerland.
[57] Takeda T, Sozen MA, Nielsen NN. Reinforced concrete response to simulated earthquakes. J Struct Div 1970;96(12):2557–73.
[58] Pegon P, Molina FJ, Magonette G. Continuous pseudo-dynamic testing at ELSA. In: Saouma VE, Sivaselvan MV, editors. Hybrid simulation; theory, implementation and applications. Taylor & Francis/Balkema; 2008. p. 79–88.
[59] Saisi A, Toniolo G. Precast r.c. columns under cyclic loading: an experimental programme oriented to EC8. Politecnico di Milano: Studies & Researches; 1999.
[60] Biondini F, Titi A, Toniolo G Pseudodynamic tests and numerical simulations on a full-scale prototype of a multi-storey precast structure. 15th WCEE 2012, Lisbon, Portugal;Paper No. 1468.
[61] Nascimbene R, Brunesi E, Bolognini D, Bellotti D. Experimental investigation of the cyclic response of reinforced precast concrete framed structures. PCI J 2015;60(2):57–79.
[62] Dal Lago A, Dal Lago B. Progetto SAFECAST: problematiche riscontrate confrontando progetto e prove sismiche. 19th CTE Congress, Bologna, Italy;553-562 [in Italian]; 2012.